AGU PUBLICATIONS

Geophysical Research Letters

RESEARCH LETTER

10.1002/2016GL071307

Key Points:

- The proxy record shows that the dominant periodicity of the glacial cycle shifts from 40 kyr to 100 kyr about a million years ago
- In a cold climate the sea ice grows asymmetrically between two hemispheres with changing Earth's orbital precession and eccentricity
- In a warmer climate, the hemispheric asymmetry of the sea ice decreases, diminishing the precession and eccentricity signatures

Correspondence to:
J.-E. Lee,
leeje@brown.edu

Citation:
Lee, J.-E., A. Shen, B. Fox-Kemper, and Y. Ming (2017), Hemispheric sea ice distribution sets the glacial tempo, *Geophys. Res. Lett.*, *44*, 1008–1014, doi:10.1002/2016GL071307.

Received 22 SEP 2016
Accepted 5 JAN 2017
Accepted article online 7 JAN 2017
Published online 27 JAN 2017

Hemispheric sea ice distribution sets the glacial tempo

Jung-Eun Lee[1], Aaron Shen[2], Baylor Fox-Kemper[1], and Yi Ming[3]

[1]Department of Earth, Environmental and Planetary Sciences, Brown University, Providence, Rhode Island, USA, [2]Center for Computation and Visualization, Brown University, Providence, Rhode Island, USA, [3]Geophysical Fluid Dynamics Laboratory, Princeton, New Jersey, USA

Abstract The proxy record of global temperature shows that the dominant periodicity of the glacial cycle shifts from 40 kyr (obliquity) to 100 kyr (eccentricity) about a million years ago. Using climate model simulations, here we show that the pace of the glacial cycle depends on the pattern of hemispheric sea ice growth. In a cold climate the sea ice grows asymmetrically between two hemispheres under changes to Earth's orbital precession, because sea ice growth potential outside of the Arctic Circle is limited. This difference in hemispheric sea ice growth leads to an asymmetry in absorbed solar energy for the two hemispheres, particularly when eccentricity is high, even if the annual average insolation is similar. In a warmer climate, the hemispheric asymmetry of the sea ice decreases as mean Arctic and Antarctic sea ice decreases, diminishing the precession and eccentricity signals and explaining the dominant obliquity signal (40 kyr) before the mid-Pleistocene transition.

1. Introduction

Paleoproxy data show that Earth's climate undergoes the glacial-interglacial cycle with semiregular periodicity, with phases strongly linked to orbital variations [*Hays et al.*, 1976; *Huybers and Curry*, 2006; *Imbrie*, 1984; *Imbrie et al.*, 1992; *Lisiecki and Raymo*, 2005]. For the past ~1 Ma, the dominant periodicity has been eccentricity (~100 kyr) embedded with precession (~21 kyr) and obliquity (~40 kyr) signals. Before ~1 Ma, the dominant signal was obliquity with weak eccentricity and precession signals [*Imbrie*, 1984; *Lisiecki and Raymo*, 2005], and this shift is called mid-Pleistocene transition. Due to the predominance of northern hemispheric glaciers, the northern hemispheric insolation is usually the assumed driver of the glacial-interglacial cycle [*Milankovitch*, 1930].

The strong signal of eccentricity (and to a lesser extent, precession) during the past 1 Myr has been puzzling because the effect of eccentricity on seasonal insolation is small [*Imbrie et al.*, 1992], although eccentricity modulates precession [*Lisiecki*, 2010]. However, it has been proposed that the 100 kyr cycle may be a modulation of the obliquity signal because the integrated seasonal insolation at a given location does not change with precession [*Huybers*, 2003, 2006]. While there are numerous studies that link paleoproxies to insolation forcings, there is yet no broadly accepted explanation for how ice ages start and why they follow a 100 kyr cycle and why the pace of the glacial cycle changes in mid-Pleistocene.

Two ideas that may be directly contrasted against the proposed mechanism are those of *Raymo and Lisiecki* [2006] and *Huybers* [2006]. *Raymo and Lisiecki* [2006] argue that the observed dominance of obliquity during the (warmer) early Pleistocene/Pliocene is due to a matched reduction in the terrestrial Antarctic ice sheet, which compensates the northern hemispheric glacial change and thereby cancels the global effect of precession and eccentricity under warmer climates. *Huybers* [2006] argues that the obliquity cycle is more important than the other cycles because the intensity and duration of the precessional signal cancel each other out (hotter summers are shorter), and *Huybers* [2003]] argues that only obliquity, not precession or eccentricity, shows a statistically significant effect on glacial termination.

Here we use the NOAA/Geophysical Fluid Dynamics Laboratory (GFDL) general circulation model [*Anderson*, 2004; *Winton*, 2003] to mechanistically understand potential causes of the 100 kyr glacial-interglacial cycle and the transition from 40 kyr to 100 kyr cycles. The Southern Hemisphere has more potential to grow sea ice in a cold climate because continental landmass surrounds the Arctic Circle, leaving little room for sea ice to grow in the Northern Hemisphere once the Arctic Ocean is frozen year-round. Sea ice growth is rapid—even seasonal; increased sea ice in the Southern Ocean affects albedo [*Budyko*, 1969], air-ice-sea fluxes [*Hunke and Ackley*, 2001; *McPhee et al.*, 1999], and CO_2 outgassing [*Ferrari et al.*, 2014; *Skinner et al.*, 2010; *Stephens and Keeling*, 2000], amplifying the initial cooling.

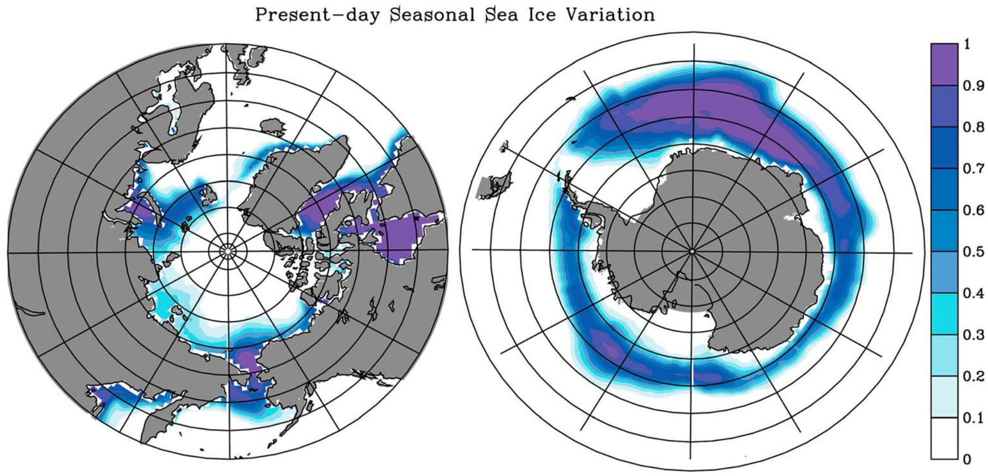

Figure 1. The seasonal difference in maximum (March for the Northern Hemisphere and September for the Southern Hemisphere) and minimum (September for the Northern Hemisphere and March for the Southern Hemisphere) sea ice extent in the (left) Northern and (right) Southern Hemispheres averaged from 1980 to 2015.

2. Method

To understand how insolation forcings influence global temperature, we performed climate model simulations by using the GFDL Atmospheric Model version 2.1 (AM2.1) [*Anderson*, 2004] with a slab ocean configuration [*Winton*, 2003], varying orbital parameters and atmospheric CO_2 concentration. The version of the model used does not include potentially significant oceanic feedback mechanism, but recent work shows that current coarse-resolution climate models may have trouble capturing these feedback mechanism [*Ferreira et al.*, 2015; *Haine et al.*, 2015; *Tomas et al.*, 2016]. The model used also does not have an active land glacier component, but it does have the ability to represent the land processes and the albedo changes due to snow and sea ice. We expect that increasing model complexity will only modulate, not eliminate, the hemispheric geometric asymmetry at the heart of our mechanism. For each orbital parameter configuration, we performed two sets of runs: one set under present-day greenhouse concentration and another set under a warmer climate to represent the environment before 1 Ma. Because simulated climate from the GFDL model tends to be colder when compared to historical temperature records, we selected a 400 ppm atmospheric CO_2 concentration with a mean temperature similar to actual global temperatures in 1950 as our present-day configuration (triangle in Figure 1d). We note that our study aims to explain the differences in the response of the sea ice under different climate regimes and not to accurately simulate the climate conditions for the Pliocene-Pleistocene. Because our simulation did not include changes in ocean circulation, glacial dynamics, or active carbon cycling, we could not capture any climate change as a result of these factors. For the same reason, the model equilibrates rapidly to the orbital forcing selected. For each simulation, we ran the model for 35 years and averaged the last 10 years for our analysis.

3. Results and Discussion

The precession of Earth's longitude of perihelion influences the insolation within each season because Earth orbits the Sun elliptically. The impact of precession is therefore opposite on the northern and southern polar regions. Whichever hemisphere is closer to the Sun in its summer, the other is further away from the Sun during its summer. Thus, the hemispheric effects will cancel out on global average if the precession response is symmetric for the Northern and Southern Hemispheres [*Raymo and Lisiecki*, 2006]. Furthermore, the precessional signal is somewhat compensated due to the negative relationship between the strength and length of a season [*Huybers*, 2006].

However, symmetry under precession is not expected, because the land-ocean configuration of the Northern and Southern Hemispheres is different, so sea ice and land ice grow differently and initiate different climate feedback. Presently, seasonal variation of the southern hemispheric sea ice is much larger than that of the northern hemispheric sea ice (Figure 1 and Table 1), influencing the seasonality of absorbed energy to

Table 1. The Total Area ($\times 10^6$ km^{-2}) of Monthly Maximum and Minimum and the Difference Between Maximum and Minimum Sea Ice Distribution [*Rayner*, 2003] Averaged From 1980 to 2015

	NH	SH
Max	13.27	16.39
Min	5.40	2.57
Difference	7.87	13.82

Earth and leaving the global climate more susceptible to the precessional cycle. There is a pronounced hemispheric pattern for seasonal changes in sea ice extent under global warming [*Eisenman et al.*, 2011]. Sea ice in the Arctic Ocean may be subject to rapid summer melting, whereas austral summertime sea ice in the Southern Ocean can only retreat as far as the Antarctic continent, which occurs at present for ice off of East Antarctica and nearly so for West Antarctica. In an environment cooler than today's, Antarctic sea ice can expand at all longitudes, whereas only about 1/6th to 1/12th of the longitudes are open to growing Arctic sea ice through Fram and Bering Straits and the Labrador and Greenland-Iceland-Norwegian Seas.

Although cumulative insolation is similar for June and December perihelion cases [*Huybers*, 2006] (black lines in Figure 2a), stronger summer insolation in December perihelion case can lead to a substantial Antarctic sea ice melt, increasing the actual energy that Earth absorbs (dotted versus solid blue lines in Figure 2a). As a result, the extent of global sea ice is larger when the southern hemispheric summer insolation is low (June perihelion; Figure 3). Increased extent of Antarctic sea ice during June perihelion induces more reflection of sunlight (high albedo), and thus, there is less net solar energy into the Earth (blue lines in Figure 2b). Due to potential mitigation of asymmetry by clouds, clear-sky regions (dotted) are contrasted against the all-sky total response (solid in Figure 2b). Absorption of the solar energy is strongly affected by precession in the clear-sky case (blue dotted line), but precession signal is still evident for the all-sky case (blue solid line) where some compensation due to cloud cover decreases the difference. The open water of the Southern Hemisphere has more area for a stronger sea ice-albedo feedback than that of the Northern Hemisphere (Figure 3), and since the Southern Hemisphere receives less solar energy during the June perihelion than during the December perihelion due

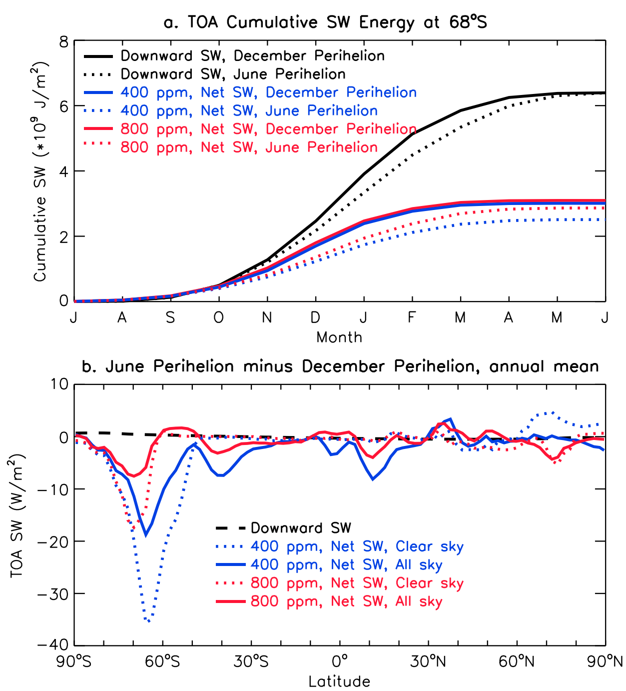

Figure 2. (a) Top of the atmosphere (TOP) cumulative shortwave (SW) energy from July at 68°S for December perihelion (solid lines) and June perihelion cases (dotted lines) and the (b) difference in net shortwave energy flux at the top of the atmosphere for the clear (dotted) and all-sky (solid) conditions from the June perihelion and to the December perihelion cases using GFDL CM2.1. The blue lines indicate the results from a CO_2 concentration of 400 ppm, and the red lines indicate the results from a CO_2 concentration of 800 ppm. The black dashed line represents downward SW energy difference. Obliquity is 23°, and eccentricity is 0.05.

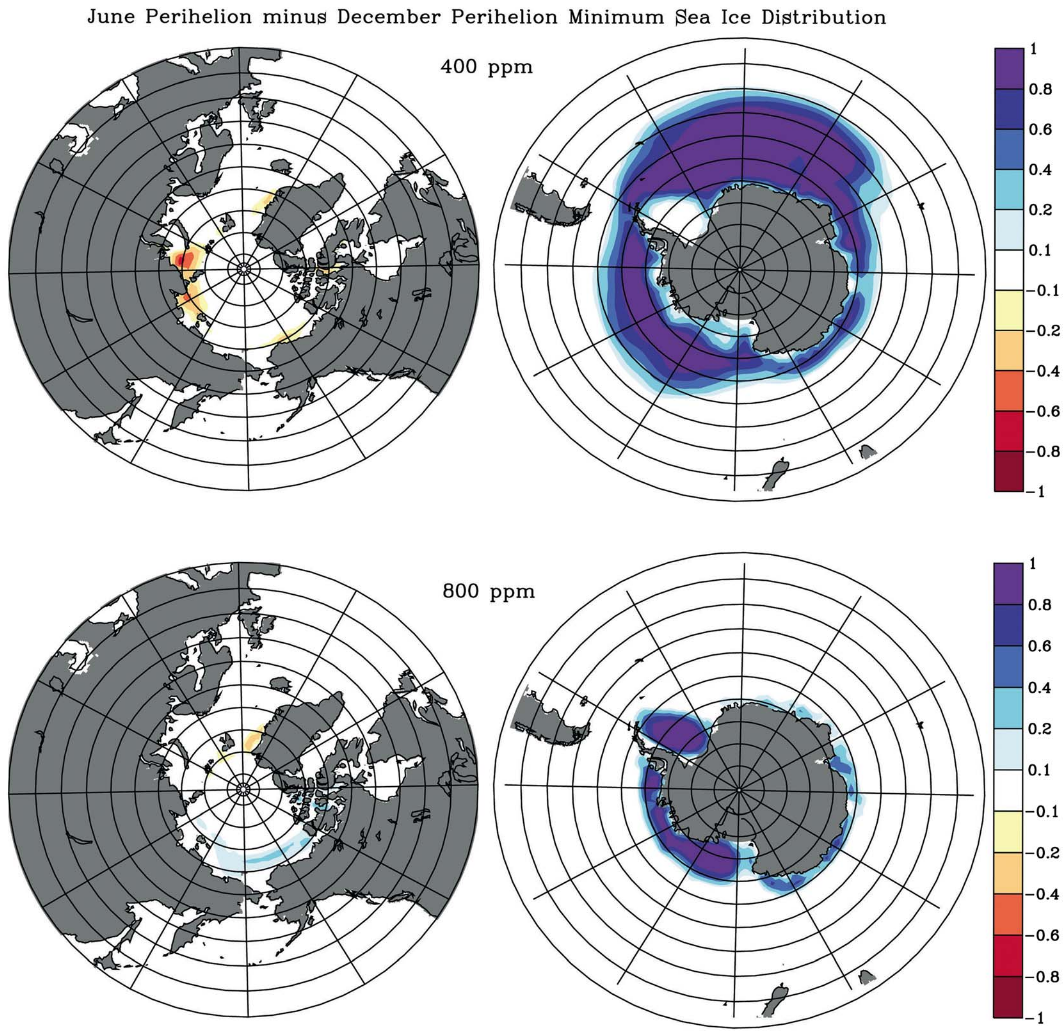

Figure 3. The difference in minimum sea ice extent (March extent for the Southern Hemisphere and September extent for the Northern Hemisphere) from the June to December perihelion using GFDL CM2.1 for (top row) 400 ppm and (bottom row) 800 ppm CO_2 concentration cases. Obliquity is 23°, and eccentricity is 0.05.

to increased sea ice, global temperature is lower during the June perihelion than during the December perihelion (Figure 4a). The global mean temperature decreases despite the increase in the northern polar insolation during its summer in the June perihelion case, because the northern sea ice energy budget feedback is weaker than the southern. Due to less sea ice overall, the asymmetrical response between two hemispheres to precession is weakened under increased concentration of atmospheric carbon dioxide (Figures 2 and 3).

The changes in insolation due to eccentricity alone with fixed precession are small as previous studies have mentioned [*Imbrie et al.*, 1992], but when coupled with precession, ellipticity effects are amplified. The degree of asymmetrical response to precession is larger with higher eccentricity (Figure 4b), and thus, we expect that the Earth's temperature rhythm will produce an eccentricity signal (100 kyr). A strong 100 kyr signal shows up in the spectral analysis because the influence of precession becomes high only when eccentricity is high. Small eccentricity leads to a small precession effect (Figure 4c). Thus, the precession signal is muted when eccentricity is low.

Obliquity affects the global temperature due to variations in latitudinal insolation [*Huybers*, 2006]. This relationship is evident in our runs varying only obliquity (Figure 4d). Global mean temperature is high under high obliquity because summer insolation increases for both polar regions, triggering the albedo feedback. Because winter insolation is almost zero near the polar region, winter insolation variability has few consequences for global temperature. Thus, we affirm the hypothesis of *Huybers* [2006] that both the Pleistocene

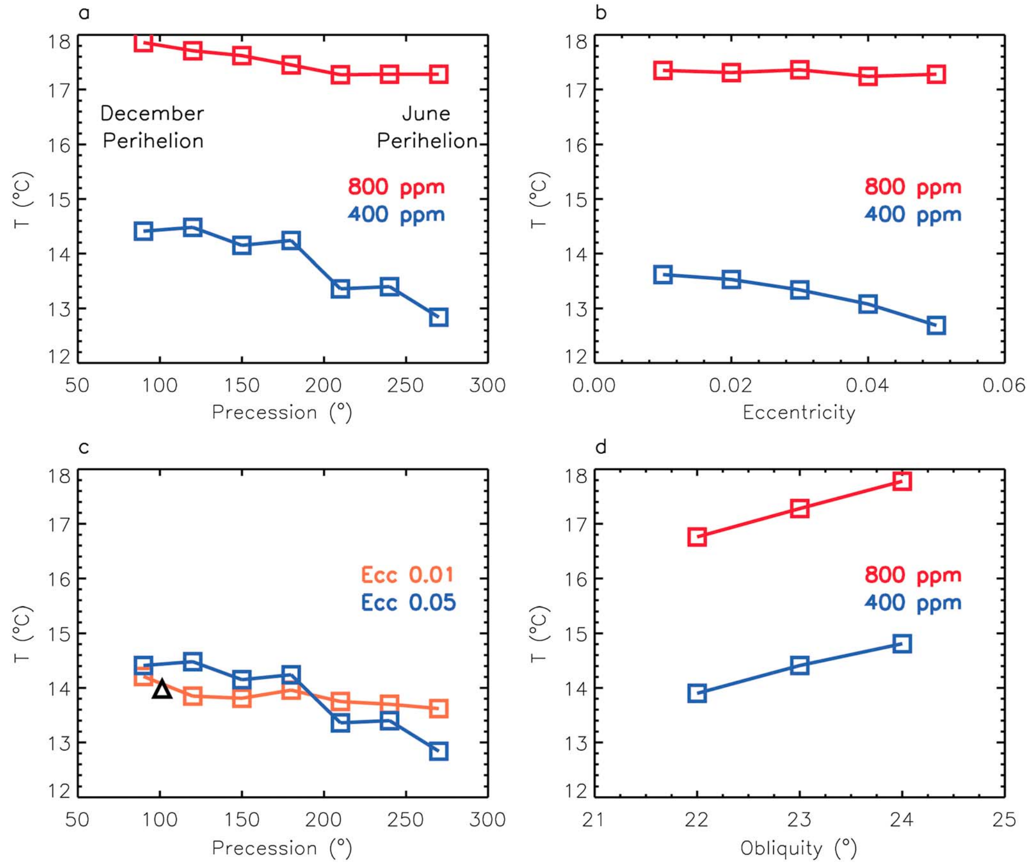

Figure 4. The relationship between global mean temperature and (a) precession in relation with vernal equinox (obliquity and eccentricity are kept constant as 23° and 0.05), (b) eccentricity of Earth's orbit around the Sun (all cases are for December perihelion with an obliquity of 23°), (c) precession of equinox (obliquity is kept constant as 23°; eccentricity varies between 0.05 and 0.01 for the orange and light blue lines), and (d) obliquity of Earth's axial tilt (all cases are for December perihelion with an eccentricity of 0.05) from GFDL AM2.1 with Slab Ocean Model. The blue lines indicate the results from a CO_2 concentration of 400 ppm, and the red lines indicate the results from a CO_2 concentration of 800 ppm. Both cases in Figure 4c are with 400 ppm CO_2. The black triangle shows the orbital parameters and global temperature in 1950, suggesting that the model has a cold bias.

and Pliocene experienced climate fluctuations with varying obliquity. Thus, while obliquity effects remain in a warmer world (Figure 4d), precession and eccentricity signals increasingly cancel between hemispheres, so the global effect decreases or disappears (Figures 4a and 4b).

Although northern hemispheric insolation has often been considered the glacial-interglacial driver since Milankovitch's proposal [*Imbrie et al.*, 1992; *Milankovitch*, 1930], several paleoproxies suggest Southern Ocean warming before terminations of ice ages or increases of CO_2 [*Collins et al.*, 2012; *Hays et al.*, 1976]. For example, high-resolution records of a Southern Ocean sea ice proxy show the maximum equatorward extension before the Last Glacial Maximum [*Collins et al.*, 2012], implying that the maximal glacial extent was a response and not the driver of southern hemispheric cooling. Additionally, simultaneous analysis of ice cores and deep ocean isotopic compositions reveal that the global ice volume, and hence the growth of northern hemispheric glaciers, follows the CO_2 increase [*Shackleton*, 2000], refuting the claim that the 100 kyr cycle may arise from ice sheet dynamics.

In an environment warmer than today's, the response to the precessional forcing is much smaller because summertime Antarctic ice will tend to be much smaller in extent (Figures 2b, 3c, and 3d). Furthermore, under warmer conditions, the Antarctic continent reduces the potential for southern hemispheric sea ice loss, while the Arctic summer losses are most apparent (as in recent decades). Thus, in a warmer climate, the asymmetry diminishes because the southern sea ice extent during the summer varies little once the summer sea ice there has diminished, leading to the dominance of the 40 kyr periodicity. *Raymo and Lisiecki* [2006] make a similar argument based on changes in land glaciers. They claim that the ablation of the East Antarctic glacier in a warmer climate compensates the change of the northern hemispheric glaciers and decreases the interhemispheric asymmetry. However, glaciers are slow to grow, so we expect that glaciers respond and may strengthen feedback in a cooling world, given the simultaneous response of the global glaciers to temperatures [*Denton et al.*, 1999; *Mercer*, 1984; *Putnam et al.*, 2013]. In contrast, sea ice change is rapid and triggers immediate feedback, which may incite glacier growth. Furthermore, our modeled sea ice change tends to drive global temperature more consistently than local temperature. Smaller-scale local responses, particularly in the polar region, may follow the local insolation signal.

Hemispheric asymmetry also decreases when eccentricity is low. Under low eccentricity, the obliquity signal is dominant. Therefore, it is no surprise that previous studies argue that glacial terminations are driven by obliquity [*Huybers*, 2003]. During times of high eccentricity, southern hemispheric insolation fluctuates with the precessional cycle and thus frequently, so the duration of warming may not be long enough for glaciers to melt completely [*Raymo*, 1997].

4. Summary and Conclusion

In this manuscript, we show that the pace of the glacial cycle depends on the pattern of hemispheric sea ice growth. In the past 1 Myr, the dominant glacial cycle has a 100 kyr periodicity because sea ice grows asymmetrically for the two hemispheres in response to the precessional cycle (~21 kyr cycle), particularly when eccentricity (~100 kyr cycle) is high, modulating absorbed solar energy to Earth, although annual mean insolation at a given location is not significantly influenced by precession or eccentricity. Our hypothesis is based on the simple land-ocean configuration of the Earth: sea ice area in the Southern Hemisphere is more variable in colder climates. While further research will be necessary to explain how the ocean circulation and land glaciers respond to the increase in sea ice, our research provides a new explanation for why the global temperatures have eccentricity and precession signals.

In a warmer climate, however, the hemispheric asymmetry of the sea ice decreases as mean Arctic and Antarctic sea ice decreases, diminishing the precession and eccentricity signals and explaining the dominant obliquity signal (40 kyr) before the mid-Pleistocene transition, about 1 Myr ago. While previous studies showed that sea ice could play a significant role in determining global temperature with varying orbital parameters [*Gildor and Tziperman*, 2001; *Kim et al.*, 1998; *Lee and Poulsen*, 2006], our hypothesis explains how sea ice distribution can modify the pace of the ice age cycle.

We note that our mechanism may not completely resolve how deglaciation is triggered. During the glacial period, icy surfaces cover both hemispheres, and thus, obliquity may be more important in determining the ice age termination [*Huybers and Wunch*, 2005]. We also do not include the dynamical response of the ocean and glaciers in our study; the dynamics of glaciers, as well as atmospheric and oceanic circulation changes, modulate the glacial-interglacial cycle. Characterizing local response is particularly difficult with our current model because the existence of glaciers tends to amplify local responses.

Our study provides how the glacial period may have started in the last million years. When the Southern Hemisphere receives an explanation of less solar energy in winter, increased sea ice in the Southern Ocean should trigger positive feedback in CO_2, energy balance, and air-ice-sea fluxes [*Ferrari et al.*, 2014; *Skinner et al.*, 2010; *Stephens and Keeling*, 2000], amplifying the initial cooling. Temperature differences arising from atmospheric CO_2 changes and energy loss will propagate globally, amplifying the cooling and leading to the growth of glaciers and the onset of an ice age [*Shackleton*, 2000].

Acknowledgments
J.E.L. acknowledges that J. Bishop suggested the title. J.E.L. thanks I. Fung, T. Schneider, M. Raymo, P. Huybers, and an anonymous reviewer for their helpful discussion on the earlier version of the manuscript. Sea ice data are from Hadley Centre Sea Ice and Sea Surface Temperature data set (http://www.metoffice.gov.uk/hadobs/hadisst/) [*Rayner*, 2003]. The study was funded by NSF 1415464, and the runs were performed on Gaia at NOAA GFDL.

References

Anderson, J. L. (2004), The new GFDL global atmosphere and land model AM2-LM2: Evaluation with prescribed SST simulations, *J. Climate*, *17*, 4641–4673.

Budyko, M. I. (1969), The effect of solar radiation variations on the climate, *Tellus*, *21*, 611–619.

Collins, L. G., J. Pike, C. S. Allen, and D. A. Hodgson (2012), High-resolution reconstruction of southwest Atlantic sea-ice and its role in the carbon cycle during marine isotope stages 3 and 2, *Paleoceanography*, *27*, PA3217, doi:10.1029/2011PA002264.

Denton, G. H., C. Heusser, T. Lowel, P. I. Moreno, B. G. Andersen, L. E. Heusser, C. Schlühter, and D. R. Marchant (1999), Interhemispheric linkage of paleoclimate during the last.

Eisenman, I., T. Schneider, D. S. Battisti, and C. M. Bitz (2011), Consistent changes in the sea ice seasonal cycle in response to global warming, *J. Climate*, *24*(20), 5325–5335, doi:10.1175/2011jcli4051.1.

Ferrari, R., M. F. Jansen, J. F. Adkins, A. Burke, A. L. Stewart, and A. F. Thompson (2014), Antarctic sea ice control on ocean circulation in present and glacial climates, *Proc. Natl. Acad. Sci. U.S.A.*, *111*(24), 8753–8758, doi:10.1073/pnas.1323922111.

Ferreira, D., J. Marshall, C. M. Bitz, S. Solomon, and A. Plumb (2015), Antarctic Ocean and sea ice response to ozone depletion: A two-time-scale problem, *J. Climate*, *28*(3), 1206–1226, doi:10.1175/jcli-d-14-00313.1.

Gildor, H., and E. Tziperman (2001), Sea ice climate switch mechanism for the 100-kyr glacial cycles, *J. Geophys. Res.*, *106*, 9117–9133, doi:10.1029/1999JC000120.

Haine, T. W. N., et al. (2015), Arctic freshwater export: Status, mechanisms, and prospects, *Global Planet. Change*, *125*, 13–35, doi:10.1016/j.gloplacha.2014.11.013.

Hays, J. D., J. Imbrie, and Shacklton (1976), Variations in the Earth's orbit Pacemaker of the ice ages, *Science*, *194*(4270), 1121-1132, doi:10.1126/Science.194.4270.1121.

Hunke, E. C., and S. F. Ackley (2001), A numerical investigation of the 1997–1998 Ronne Polynya, *J. Geophys. Res*, *106*(C10), 22,373–22,382, doi:10.1029/2000JC000640.

Huybers, P. (2003), Rectification and precession signals in the climate system, *Geophys. Res. Lett.*, *30*(19), doi:10.1029/2003GL017875.

Huybers, P. (2006), Early Pleistocene glacial cycles and the integrated summer insolation forcing, *Science*, *313*(5786), 508–511, doi:10.1126/science.1125249.

Huybers, P., and W. Curry (2006), Links between annual, Milankovitch and continuum temperature variability, *Nature*, *441*(7091), 329–332, doi:10.1038/nature04745.

Huybers, P., and C. Wunch (2005), Obliquity pacing of the late Pleistocene glacial terminations, *Nature*, *434*, 491–494.

Imbrie, J. (1984), On the structure and origin of major glaciation cycles 1. Linear responses to Milankovitch forcing, *Paleoceanography*, *7*, 701–738, doi:10.1029/92PA02253.

Imbrie, J., A. Berger, E. Boyle, S. Clemens, A. Duffy, W. Howard, G. Kukla, J. Kutzbach, D. Martinson, and A. A. O. McIntyre (1992), On the structure and origin of major glaciation cycles 2. The 100,000-year cycle, *Paleoceanography*, *7*, 701–738, doi:10.1029/92PA02253.

Kim, S.-J., T. J. Crowley, and A. Stossel (1998), Local orbital forcing of Antarctic climate change during the last interglacial, *Science*, *280*, 728–730.

Lee, S.-Y., and C. J. Poulsen (2006), Sea ice control of Plio-Pleistocene tropical Pacific climate evolution, *Earth Planet. Sci. Lett.*, *248*(1–2), 253–262, doi:10.1016/j.epsl.2006.05.030.

Lisiecki, L. E. (2010), Links between eccentricity forcing and the 100,000-year glacial cycle, *Nat. Geosci.*, *3*(5), 349–352, doi:10.1038/ngeo828.

Lisiecki, L. E., and M. E. Raymo (2005), A Pliocene-Pleistocene stack of 57 globally distributed benthic δ18O records, *Paleoceanography*, *20* PA1003, doi:10.1029/2004PA001071.

McPhee, M. G., C. Kottmeier, and J. H. Morison (1999), Ocean heat flux in the central Weddell 1999, *J. Phys. Oceanogr.*, *29*, 1166–1179.

Mercer, J. H. (1984), Simultaneous climatic change in both hemispheres and similar bipolar interglacial warming: Evidence and implications, in *Climate Processes and Climate Sensitivity*, *Geophys. Monogr.*, vol. 29, edited by J. Hansen and T. Takahashi, pp. 307–313, AGU, Washington, D. C.

Milankovitch, M. (1930), in *Handbuch der Klimatologie*, edited by W. Koppen and R. Geiger, pp. 1–176, Gebruder Borntraeger, Berlin.

Putnam, A. E., J. M. Schaefer, G. H. Denton, D. J. A. Barrell, S. D. Birkel, B. G. Andersen, M. R. Kaplan, R. C. Finkel, R. Schwartz, and A. M. Doughty (2013), The Last Glacial Maximum at 44°S documented by a 10Be moraine chronology at Lake Ohau, Southern Alps of New Zealand, *Quat. Sci. Rev.*, *62*, 114–141, doi:10.1016/j.quascirev.2012.10.034.

Raymo, M. E. (1997), The timing of major climate terminations, *Paleoceanography*, *12*(4), 577–585, doi:10.1029/97PA01169.

Raymo, M. E., and L. E. Lisiecki (2006), Plio-Pleistocene ice volume, Antarctic climate, and the global d18O record, *Science*, *313*, 492–495.

Rayner, N. A. (2003), Global analyses of sea surface temperature, sea ice, and night marine air temperature since the late nineteenth century, *J. Geophys. Res.*, *108*(D14), doi:10.1029/2002JD002670.

Shackleton, N. J. (2000), The 100,000-year Ice-Age cycle identified and found to lag temperature, carbon dioxide, and orbital eccentricity, *Science*, *289*, 1897–1902.

Skinner, L. C., S. Fallon, C. Waelbroeck, E. Michel, and S. Barker (2010), Ventilation of the deep Southern Ocean and deglacial, *Science*, *328*, 1147–1151.

Stephens, B. B., and R. F. Keeling (2000), The influence of Antarctic sea ice on glacial-interglacial CO2 variations, *Nature*, *404*, 171–174.

Tomas, R. A., C. Deser, and L. Sun (2016), The role of ocean heat transport in the global climate response to projected Arctic sea ice loss, *J. Climate*, *29*(19), 6841–6859, doi:10.1175/jcli-d-15-0651.1.

Winton, M. (2003), On the climatic impact of ocean circulation, *J. Climate*, *16*, 2875–2889.